VIII International Conference on Fracture Mechanics of Concrete and Concrete Structures
FraMCoS-8
J.G.M. Van Mier, G. Ruiz, C. Andrade, R.C. Yu and X.X. Zhang (Eds)

DESCRIPTION OF NEAR-TIP FRACTURE PROCESSES IN STRAIN HARDENING CEMENTITIOUS COMPOSITES USING IMAGE-BASED ANALYSIS AND THE COMPACT TENSION TEST

EDUARDO B. PEREIRA[1], GREGOR FISCHER[2] AND JOAQUIM A.O. BARROS[1]

[1] ISISE – University of Minho
Department of Civil Engineering, School of Engineering
Guimaraes, Portugal
E-mail: eduardo.pereira@civil.uminho.pt, barros@civil.uminho.pt
web page: http://www.uminho.pt

[2] Technical University of Denmark
Department of Civil Engineering
Brovej, bygn. 118, Lyngby, Denmark
Email: gf@byg.dtu.dk - Web page: http://www.dtu.dk

Key words: Fiber Reinforced Cementitious Composites, tension, crack initiation, crack propagation, fracture processes.

Abstract: The cracking mechanisms assume a key role in the composite behavior of Strain Hardening Cementitious Composites (SHCCs). Due to their importance, in previous studies the mechanical behavior of SHCC materials, as well as of other strain softening fiber reinforced cementitious composites, was characterized under eccentric tensile loading using the Compact Tension Test (CTT). The present research further extends this investigation, with particular emphasis on cementitious composites reinforced with multiple types of fibers. The experimental tensile load-displacement results are discussed and compared to the numerically derived responses. Furthermore, the crack initiation and propagation at the early stages of the loading sequence are analyzed. The size of the specimens and the resolution of the digital images acquired allow the detection of relatively small displacements and crack openings. The results are discussed, with special emphasis on the topology of the cracks obtained near the crack tip and on the description of the fracture process zone.

1 INTRODUCTION

The recent use of discrete micro-fibers as reinforcement in cementitious composites led to the development of materials with substantial energy dissipation ability and considerable tensile ductility. These materials aim at mitigating the limitations of conventional concrete deriving from its quasi-brittle nature, often revealed by the catastrophic collapse of structures during extreme loading events or the early loss of functional properties of structures due to insufficient durability.

Distinct design approaches have been suggested to the development of different types of Strain Hardening Cementitious

Composites. Engineered Cementitious Composites (ECC) have assumed particular relevance as a representative class of cement based materials with enhanced tensile ductility. These materials show relatively high tensile strain hardening ability (between 3% and 7% of ultimate tensile strain) with average tensile strengths of 5 MPa [1].

The mechanical behavior of SHCC is the result of a delicate balance of multiple factors. The interfacial bonding and fiber pull-out properties, the material parameters of the fibers and of the matrix, the distribution of material flaw sizes in the matrix, the fiber orientation and their dispersion in the matrix play an important role in the resulting composite mechanical behavior. The study of the influence of all these parameters separately is difficult, since they perform in a highly coupled manner. At a smaller scale, the fiber pull-out tests are often carried out to study the interaction between the single fiber and the matrix. At a larger length scale, the direct tension test using dumbbell-shaped or coupon specimens is typically utilized to characterize the tensile behavior of SHCC [2,3]. The tensile stress-strain response is thereby assessed, as well as the potential of the material to develop multiple cracks for increasing elongation. Although with additional uncertainty, inverse analysis is often alternatively used to derive indirectly the tensile stress-separation law from bending or diametric compression tests, like the Compact Tension Test (CTT), the Wedge Splitting Test (WST), the Four Point Bending Test and the Brazilian Compression test among others (see for example [4]).

The unique pseudo-strain hardening behavior observed in tensioned SHCC members is the outcome of a careful design of the composite, considering both the matrix fracture properties and the bridging effect provided by the fibers. The steady-state crack propagation mode, typically considered as an underlying concept of the multiple cracking ability of SHCC, requires the fulfillment of two design requirements, one mechanical and the other energetic. The mechanical requisite determines that the maximum bridging stress provided by the fiber reinforcement should exceed the matrix tensile strength. The energetic requirement determines that the critical complimentary energy observed in the fiber bridging stress-crack opening relationship should exceed the matrix toughness. These two design requirements emphasize the importance that the crack propagation mode and the fiber bridging stress-crack opening relationship have on the tensile behavior of SHCC [2]. The detailed characterization of the fracture process and crack propagation in these composites is, therefore, relevant to the further understanding of the composite behavior of SHCC in tension. In addition, the characterization of the bridging stress-crack opening relationship is essential to the optimal design of SHCC materials.

The characterization of the tensile behavior of SHCC based on the assessment of the tensile stress-crack opening response has been explored in previous studies [5,6]. The most relevant mechanical parameters of the composite behavior in tension are revealed by the tensile stress-crack opening relationship in a clear and objective manner. In this research the single crack tension test (SCTT) setup is used to assess the tensile stress-crack opening response of the different composites considered. These responses are subsequently used to predict the load-deformation responses obtained with a different type of test, in this case the compact tension test (CTT). The results obtained with a numerical model constructed to simulate the CTT responses are compared with the experimental results.

1.2 Digital image analysis of the cracking process

The understanding of the micro-cracking mechanisms taking place near the tip of propagating cracks is important to the further understanding of the tensile behavior of SHCCs. The research described in the literature towards the better understanding of the fracture process zone in cement-based matrix composites involves the development of special techniques particularly dedicated to the analysis of cracking. Typically the very

fine cracks to be detected require high resolution equipments [7]. In addition, most of the intrusive characterization techniques used in other materials potentially induce preliminary cracking in concrete, either due to direct mechanical action, induced drying, or the alteration of other physical variables important for the delicate balance of the microstructure of concrete. Many different techniques have been especially developed to the analysis of the fracture process zone and cracking in concrete and other cement based materials. Radiography (x-rays, neutrons, or others), dye impregnation, acoustic emission, ultrasound, laser holography and interferometry are examples of techniques utilized in the past to obtain quantitative information about the fracture process zone [7]. Although most of the macroscopic features of cracking process in concrete are well understood, the micro-mechanisms of cracking and the essence of the fracture process zone are still uncertain.

Recent developments in digital imaging technology have led to considerable improvements in the quality of the images digitally acquired, mostly considering their application to scientific research. Taking advantage of these developments, the digital image correlation technique has emerged as a valid procedure to the derivation of the full field surface displacements and strains of objects under load. This technique is based on the comparison of two digitized images of the surface of an object, before and after deformation [8]. In this study the cracking processes of the investigated cementitious composites was characterized using this image-based technique. The purpose was to identify important features of the cracking process at the surface of the specimen, and use this information to support the interpretation and discussion of the CTT mechanical results obtained. Furthermore, the characterization of the fracture processes and crack propagation in the composites near the tip of the propagating cracks, in particular at the fracture process zone (FPZ), is necessary to further describe the phase interaction during the fracture processes and crack propagation, as well as to further understand how these processes affect the tensile behavior of SHCC materials.

2 MATERIALS

The tensile behavior of four different fiber reinforced cementitious composites was investigated. Both single fiber type and hybrid fiber reinforcements were considered. Fibers of two different natures were used: PVA (polyvinyl alcohol) and PAN (polyacrylnitrile). The main properties of the fibers used are presented in Table 1.

Table 1: Main properties of the fibers.

Fiber	Tensile strength	Length	Diameter
	MPa	mm	μm
PVA	1600	8	40.0
PAN	826	6	12.7

Two different compositions of the cementitious matrix were adopted, A and B, as shown in Table 2.

Table 2: Weight proportions of the materials used in each composite, per unit weight of cement.

Matrix	Cement	Fly ash	Fine sand	Quartz powder	Water
A	1.0	2.0	0.35	0.35	0.75
B	1.0	6.0	0.0	0.0	1.40

The cementitious matrix type and the volume fraction of each fiber adopted in the composites are presented in Table 3. Two single fiber type and two hybrid fiber reinforcement composites were investigated.

Table 3: Matrix type and fiber volume fractions adopted in all composites.

Composite	Matrix type	Volume fractions (%)	
		PVA	PAN
PVA_A	A	2.0	0.0

PAN_B	B	0.0	2.0
Hyb_A	A	1.0	1.0
Hyb_B	B	1.0	1.0

3 COMPACT TENSION TEST (CTT)

3.1 Testing procedure

The Compact Tension specimen is typically used to characterize the propagation of cracks and other fracture properties in metals [9]. This specimen geometry was adapted to characterize the initiation and propagation of cracks in SHCC. The depth of the specimen was minimized to approximate the plain stress conditions. The testing procedure consisted on applying an eccentric tensile load to a single-edge notched specimen, at a constant displacement rate of 5 μm/s, to induce the initiation of a single crack and allow its propagation in a controlled manner. The dimensions and geometry of the specimen are presented in Figure 1. Further details about the testing procedure may be found in previous studies [10,11].

The formation and propagation of the tensile crack was traced at the surface of the specimens using a high resolution digital camera, positioned 90 mm away from the specimen. The 60 mm focal length lens allowed the observation of a 24 mm by 36 mm area at the surface of the specimen (see Figure 2). Images with 24 megapixel of resolution were captured every second, during the entire loading sequence. These images were subsequently used to continuously interpolate the displacement fields at the inspected surface of the specimen.

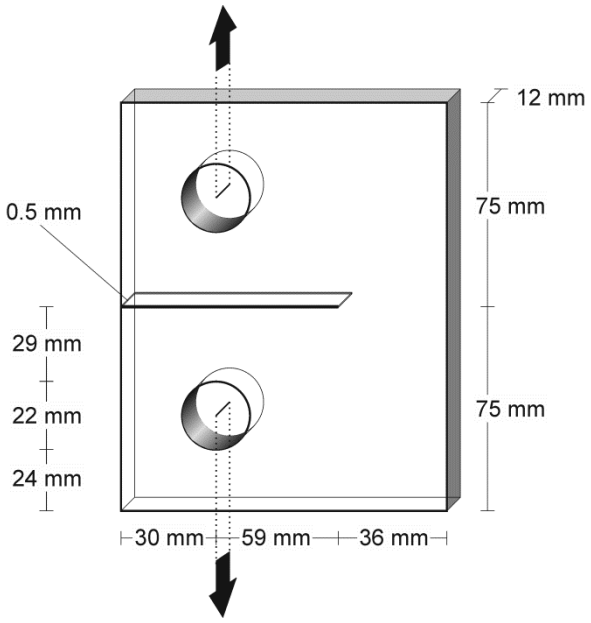

Figure 1: Geometry of the CTT specimen.

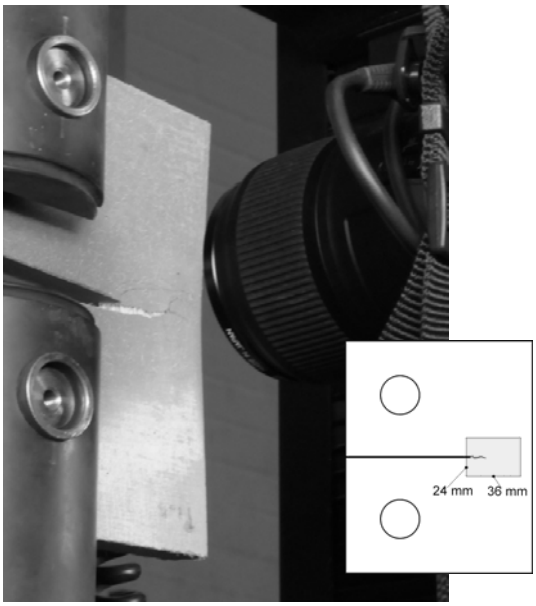

Figure 2: Image of the test-setup and identification of the observed region in the specimens.

3.2 CTT load-displacement responses

The experimental responses obtained for the composites PVA_A, PAN_B, Hyb_A and Hyb_B in terms of the tensile load versus the displacement are presented in Figure 3. For comparison, in Figure 4 the average responses of each composite are presented. These responses were obtained by averaging the tensile loads measured in the three specimens of each composite at every displacement level.

In general, the CTT tensile load-displacement responses obtained show that the different fibers used resulted in substantially different load-displacement responses. Although the peak loads reached in the different composites were not very different (between 250 N and 350 N), the displacement at which the peak loads were reached were clearly distinct, of approximately 0.25 mm in the case of the hybrid composites, 0.5 mm in the case of the PAN_B and 2 mm in the case of the PVA_A.

The detailed analysis of the results obtained with the image-based analysis showed that cracking starts early, at tensile loads not exceeding 150 N. Although this analysis will be further discussed in a subsequent section, for now, it is important to remark that the fiber contribution to restrain crack propagation is affecting the load-displacement responses since very small displacements.

When observing the measured tensile load-displacement responses of the four composites, differences can be identified between the overall behavior and shape of the curves obtained for the single fiber type and the hybrid fiber reinforced composites. In general, the hardening-softening sequences observed in the load-displacement responses reveal that there is a different range of displacements at which each fiber type is more effective. In the case of the hybrid fiber reinforced composites, the load-displacement responses reflect the different nature of the two types of fibers in the composite. This effect will be further explored in the subsequent section, where the influence of the fiber and matrix properties on the tensile responses is discussed.

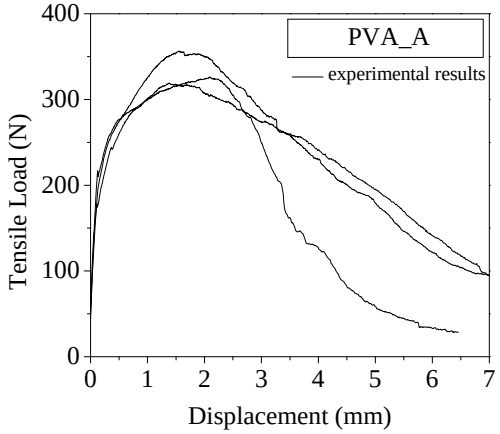

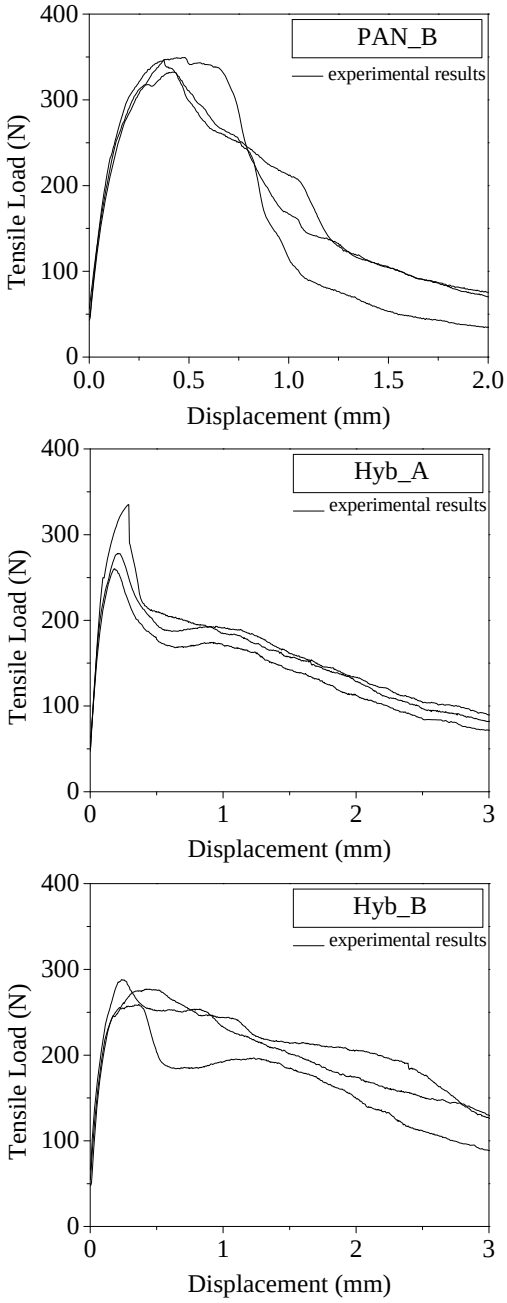

Figure 3: Load-displacement responses of the four composites tested.

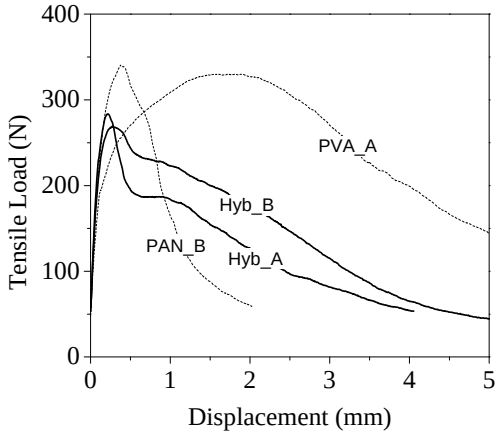

Figure 4: Average load-displacement responses of the four composites tested.

4 SINGLE CRACK TENSION TEST (SCTT)

4.1 Testing procedure

The experimental characterization of the fiber bridging effect during the crack initiation and propagation in strain hardening cementitious composites requires the formation of a single crack during the entire loading sequence. SHCC materials are designed to develop multiple cracks in tension, consequently the formation and propagation of a single crack is counteracted by the material mechanics. The requirements to guarantee the formation of a single crack in SHCC materials during tensile testing were investigated in previous studies [5]. The specimen geometry and dimensions used are presented in Figure 5.

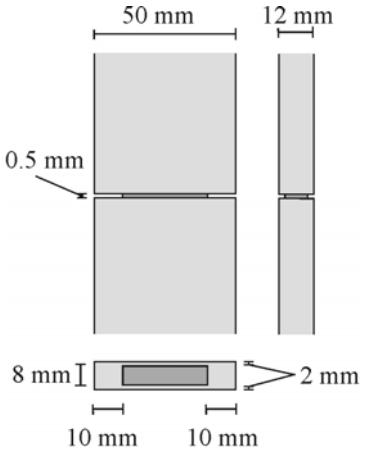

Figure 5: Specimen geometry used in the SCTT.

The length of the specimen was 120 mm and the free distance between the fixed ends during testing was 70 mm. The specimen was subjected to a constant axial displacement rate of 5 μm/s. This deformation rate was transmitted by the hydraulic actuator to the specimen by means of two hydraulic grips, providing fixed support conditions to both ends of the specimen (rotations and transverse displacements were restrained).

4.2 SCTT results

The results obtained from six specimens of each composite are presented in Figure 6. The values of the tensile stress (nominal tensile stress) were obtained by computing the ratio between the experimental tensile load and the net area of the notched cross-section (8×30 mm2). The CMODs were obtained by averaging the displacements measured in the two opposite clip gages placed at the notch.
As shown in Figure 6, the dispersion of results obtained for all four composites was reasonably low. The robust tensile responses obtained clearly showed that the different fiber reinforcements and matrices used resulted in substantially different tensile responses. The first cracking stress, the peak bridging stress, the crack opening at peak bridging stress [5] and other important composite parameters were significantly influenced by the matrix properties and fiber types combined in each composite. The activation of the PVA and the PAN fibers occurred at different stages of the cracking process. The PAN fibers, with a smaller diameter, were activated even before the first cracking stress was reached, and have contributed effectively to increase the first cracking stress. Their early effective activation was likewise followed by the early exhaustion of their contribution to restrain cracking at the post-cracking stage. In contrast, the contribution of PVA fibers to the first cracking stress was less significant. However, their contribution to restrain crack propagation was revealed mostly at later stages, by a broad tensile hardening stage initiating after the load drop that follows the first cracking stress, for a tensile stress of approximately 3.5 MPa, and

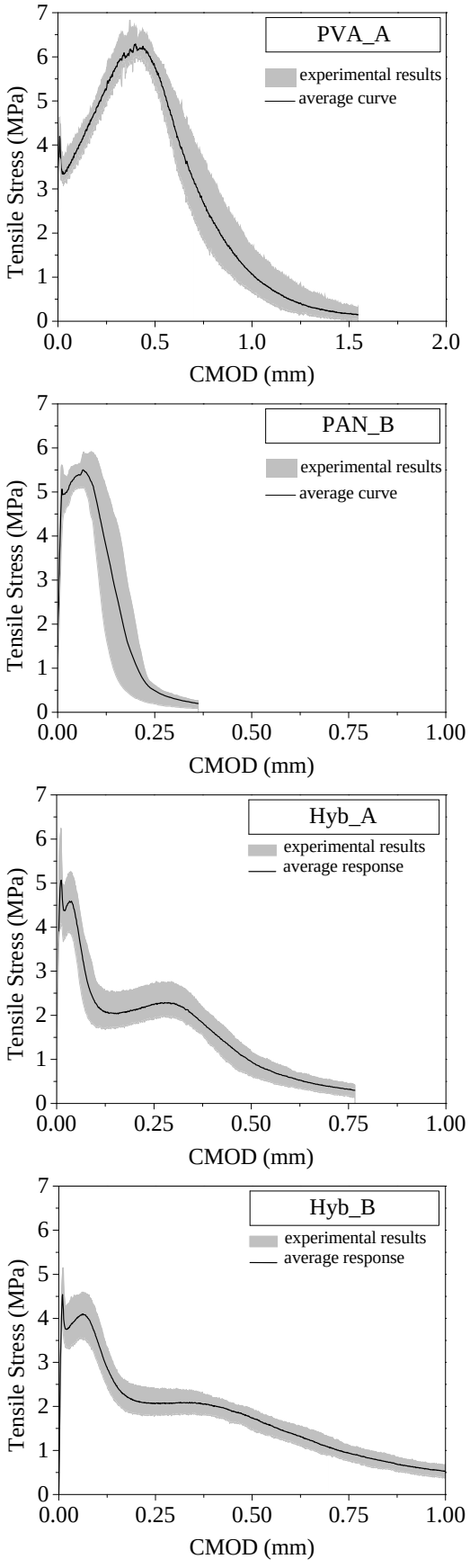

Figure 6: Tensile stress-crack opening responses of the four composites tested.

continues up to when the peak bridging stress is reached, at a tensile stress of approximately 6.2 MPa. Further discussion regarding the significance of each stage of the tensile stress-CMOD responses obtained with the SCTT may be found in previous work [5,6].

Comparing the SCTT responses obtained for the two hybrids with the ones of the two single fiber reinforced composites, a substantial difference in the shape of the tensile stress-crack opening responses was observed. In fact, the existence of two different types of fibers in the hybrid composites resulted in two distinct bridging stress peaks. The different CMOD ranges at which each fiber type was producing an optimal contribution to restrain crack propagation resulted in a multiple-peak type of tensile stress-crack opening response [6].

The effect of the matrix composition on the tensile stress-crack opening responses of the hybrid fiber reinforced composites is evaluated in Figure 7. The matrix type A led to the increase of the two peak bridging stresses. In addition, both bridging stress peaks were reached at lower CMODs. The general increase of the CMODs obtained at each load when the matrix type was altered to B were probably the consequence of a reduction of the number of rupturing fibers during matrix fracture, as a consequence of the lower matrix toughness. In addition, the greater amount of cement used in the case of matrix type A may explain both the higher peak bridging stresses and the earlier fiber rupture, due to the improvement of the fiber-matrix interface.

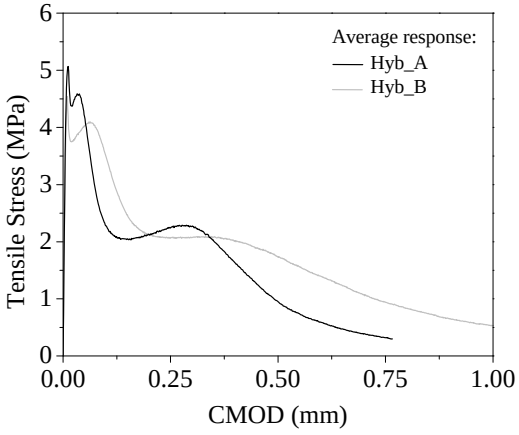

Figure 7: Average responses of the two hybrids.

5 NUMERICAL SIMULATION OF THE CTT RESPONSES

The SCTT tensile responses provide information about the composite tensile behavior when a single crack is considered. The initiation of the crack is determined mostly by the geometry of the specimen and the shape of the notched section. The slender notches and the strong section reduction adopted contribute to alter locally the stress fields and increase substantially the stress intensity at the notch tip. Therefore, the SCTT tensile responses obtained are predominantly determined by the specimen geometry until the crack is fully formed. After the full formation of the crack the fibers remain as the single links between the opposite faces of the open crack. From this stage onwards it can be assumed that the measured tensile load is exclusively the result of the fiber bridging effect. The fiber bridging stress-CMOD relationship of a certain composite is therefore evaluated objectively after the crack is fully formed. This information can be used to describe the constitutive behavior of the material in tension in terms of the tensile stress, σ_t, as a function of the crack width, δ. To verify this possibility, a finite element model of the CTT was constructed.

As shown in Figure 8, the geometry of the specimen and testing boundary conditions were modeled assuming plane stress conditions. The load was transmitted to the specimen at the two circular openings shown in Figure 8. The model was constructed using elastic 3-node triangular elements. The high geometrical gradients close to the notch tip were overcome with the considerable increase of the number of elements in this region. The young modulus, *E*, assigned to the elements was 20 GPa and the Poisson coefficient, ν, was 0.2. One layer of interface elements was placed at the ligament region (x = 75 mm, Figure 8). The interface elements were assigned with a traction-separation law, $\sigma_t = f(\delta)$, directly derived from the results obtained with the SCTT of each composite. These laws correspond to the responses shown in Figure 6, when the portion of the response prior to the attainment of the first cracking stress is removed. In this case the average tensile stress-crack opening responses obtained from the SCTT of each composite were utilized (Figure 6).

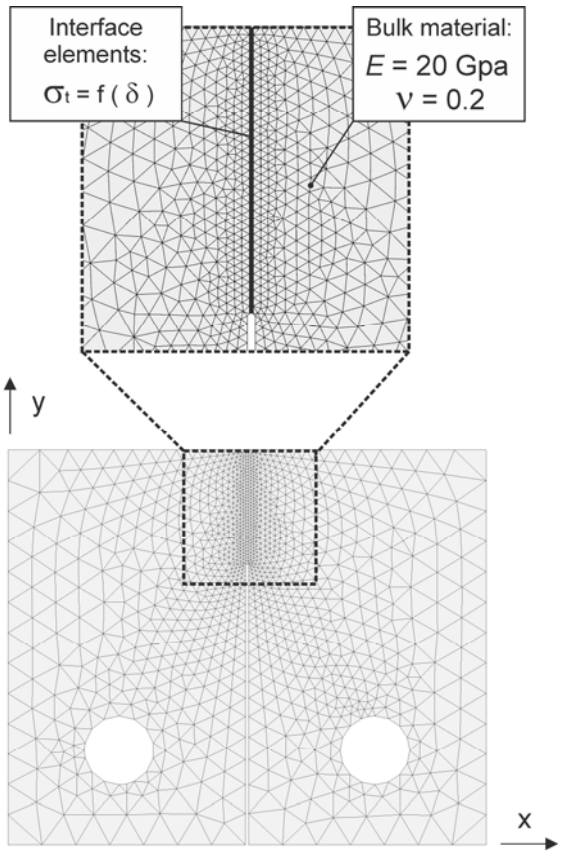

Figure 8: FEM mesh and material properties assigned to the bulk material and ligament region.

The numerical tensile load-displacement responses obtained for each composite are compared with the experimental results in Figure 9. The general shapes of the simulated CTT responses are essentially identical to the experimental ones. The peak load is well estimated in the case of the Hyb_A and slightly overestimated in the case of the Hyb_B. The displacements are also well estimated in the initial stage of the loading sequence, and become underestimated once the displacements of 0.5 mm (Hyb_A) and 1.0 mm (Hyb_B) are reached. The formation of multiple cracks at later stages of the loading sequence may justify this result. This possibility will be further explored in the subsequent section.

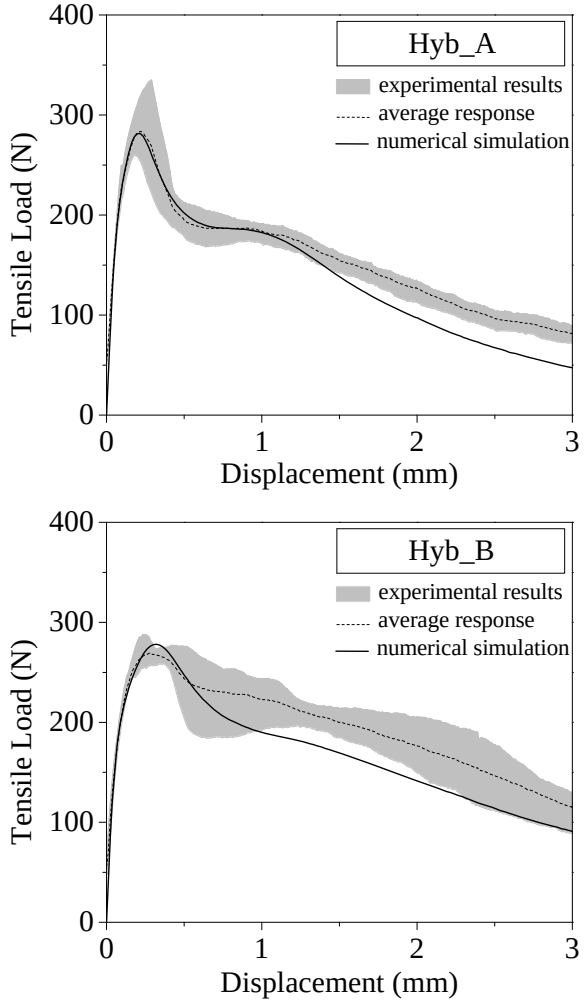

Figure 9: Experimental results and numerical responses obtained for Hyb_A and Hyb_B.

The mechanical behavior reproduced by the finite element model assumes that a single crack is formed during the entire loading sequence, and the path of this crack is set by the interface elements. The formation of more than one crack results in the increase of the displacement at the same load. In addition, when more than one crack is formed, the rupture of the specimen will be eventually determined by the 'weakest' crack, or the crack showing the lowest peak bridging stress (the weakest link principle). The peak load overestimation may therefore be the result of both the assumption of a single crack forming in the numerical model and the adoption of the average tensile stress-CMOD behavior to derive the stress-separation law of the interface elements.

5 IMAGE-BASED ANALYSIS OF THE CRACKING PROCESS

The detailed analysis of the crack patterns generated at the surface of the specimens confirmed that more than one crack was formed (Table 4). The stage one was selected in all specimens to show the last stage at which no cracks were detected. All selected stages are identified in Figure 10.

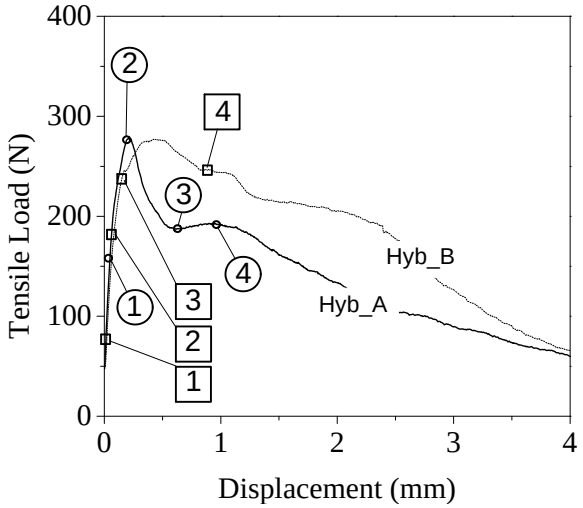

Figure 10: Experimental load-displacement responses of the imaged specimens and identification of the selected stages shown in Table 4.

Considering the Hyb_A specimen, the second stage selected shows the crack pattern obtained when the peak load was reached. The third stage selected shows the crack pattern obtained when the load reaches the local minimum, before entering the second mild hardening sequence. The fourth stage selected refers to the instant at which the second peak load was reached. From this stage onwards new crack branches only form at the crack tips near the edge of the specimen on the right, with the further opening of the main cracks previously formed.

Considering the Hyb_B specimen, the selected stage two shows the last stage up to which only one crack was visible. After this a second crack initiates at the tip of the notch and propagates at the center of the specimen, as shown in selected stage three. From stage three onwards more cracks form parallel to the existing ones, as well as additional crack branches. The fourth stage selected refers to

St.	HYB_A	HYB_B
1		
2	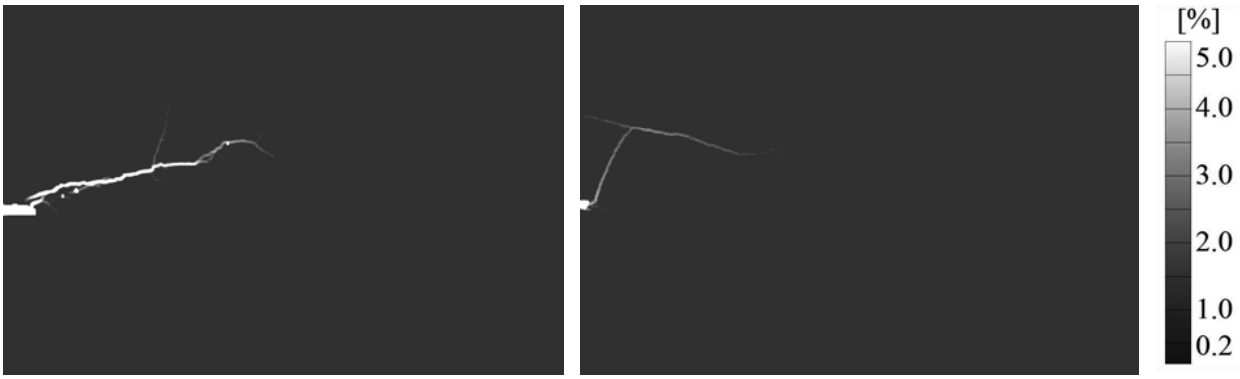	
3	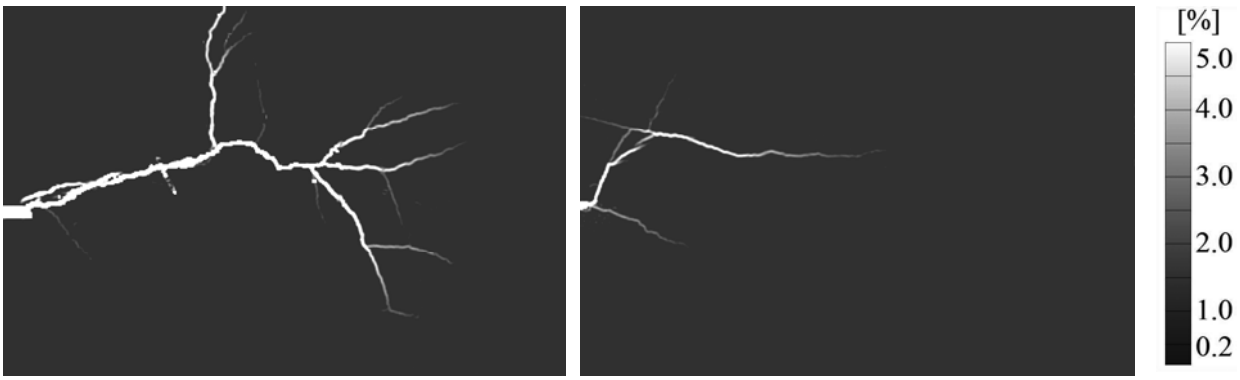	
4	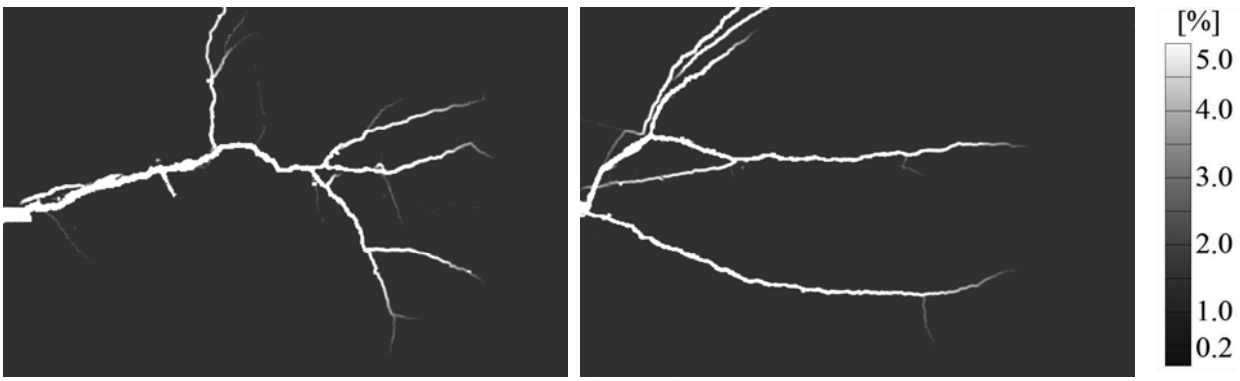	

Table 4: Selected stages of the image-based displacement analysis of Hyb_A and Hyb_B.

the instant at which the second peak load was reached. As previously observed, from this stage onwards new crack branches only form at the crack tips near the edge of the specimen on the right, with the further opening of the main cracks previously formed. Stage four also marks the stage at which the experimental and the numerical responses start to mildly diverge.

As shown in Table 4, the cracks forming in the specimens suggest that the mechanical behavior reproduced by the numerical model differs from the one experimentally obtained. The main cracks divert from its horizontal path early, while multiple crack branches form. The substantial alteration of the structural behavior caused by this early crack diverting, in opposition to the assumed single horizontal crack in the numerical model, explains partly the differences observed between the numerical simulations and the experimental results.

As discussed previously, the matrix composition used in Hyb_B leads to lower matrix toughness and lower matrix cracking strength. These two effects probably lead to a reduction of the number of fibers breaking, both at the onset of cracking and at later stages of the cracking process. In addition, the lower matrix cracking stress also increases the potential to the formation of multiple cracks. Considering that, after cracking, the fiber bridging stress build up leads to a similar increase in the ambient tensile stresses for both hybrids, the likelihood of multiple crack formation increases with the decrease of the matrix cracking stress. In fact, when observing the results obtained for Hyb_A on Table 4, the formation of crack branches that originate at the principal crack seems to prevail. In contrast, for Hyb_B multiple cracks originate at the tip of the notch. These cracks, while propagating in a predominantly horizontal direction, are in essence different from the typical crack branches propagating in a predominantly vertical direction observed in the Hyb_A composite. These essentially different cracking processes observed in both hybrids may be explained by the different significance that the two main micromechanical aspects of the composite tensile behavior are assuming in each composite. These are the fiber bridging capacity resulting of the fiber reinforcement, and the toughness of the matrix that conditions fracture mechanisms.

6 CONCLUSIONS

This investigation focused on the initiation and propagation of cracks in SHCC materials, considering the compact tension test (CTT) and cementitious composites reinforced with two different types of fibers. Different characteristic tensile load-displacement behaviors were obtained, as a result of the different geometry and properties of the fibers used. Although the geometry of the specimen and the test setup configuration were defined to create the necessary conditions to the initiation of a single crack, the results obtained with the image-based analysis have shown that multiple cracks were forming. The processed images of the surface of the specimens revealed disordered crack patterns that were significantly different from the ones that were suggested by the simple visual inspection. These results were critical to the understanding of the mechanical responses obtained, as well as to identify different micro-mechanical aspects of the cracking process that resulted from the different stiffness of the two types of cementitious matrix adopted. Essentially two distinct crack propagation mechanisms were identified. These types were shown to be directly related to the strain hardening potential of each cementitious composite and the related multiple crack formation ability. The same hybrid fiber reinforcement combined with the two different cementitious matrices has undergone the transition between a cracking process where the formation of essentially vertical crack branches was predominant, to a cracking process where multiple horizontal cracks were initiating at the tip of the notch and propagating throughout the specimen.

The characterization of the tensile stress-crack opening behavior of the four cementitious composites using the single crack

tension test (SCTT) has shown that the different fibers used are more effective at crack restraining for different crack openings. This difference results in a multiple-peak shape of the post-cracking responses observed in n the hybrid fiber reinforced composites. The tensile stress-crack opening responses obtained with the SCTT were used to predict the tensile load-displacement behaviors obtained with the CTT. Although a good general agreement between the numerical and experimental results were obtained, the peak load was somewhat overestimated in some cases and the deformations slightly underestimated by the numerical model. The results obtained with the image-based analysis explain the deviation between the numerical and the experimental results. The identified cracking patterns indicate a mechanical response that different from the one assumed in the numerical model.

ACKNOWLEDGMENTS

The authors thank the Portuguese National Science Foundation for the financial support, through grant SFRH / BD / 36515 / 2007, funded by POPH - QREN, the Social European Fund and the MCTES, and DTU-Byg for their support of the work as part of this project.

REFERENCES

[1] Li, V.C., "On engineered cementitious composites (ECC) - A Review of the Material and Its Applications" *J Adv Conc Tech* **1**(3): 215-230 (2003).

[2] Kanda, T., Li, V.C., "Practical design criteria for saturated pseudo strain hardening behavior in ECC." J *Adv Conc Tech* **4**(1):59-72 (2006).

[3] Naaman, A.E. and Reinhardt, H.W., "Proposed classification of HPFRC composites based on their tensile response." *Mat Struct* 39:547–555 (2006).

[4] Shah, S.P., Swartz, S.E. and Ouyang, C., *Fracture mechanics of concrete: applications of fracture mechanics to concrete, rock, and other quasi-brittle materials*, John Wiley & Sons Inc, New York (1995).

[5] Pereira, E.B. and Fischer, G. and Barros, J.A.O. "Direct assessment of tensile stress-crack opening behavior of Strain Hardening Cementitious Composites (SHCC)" Cem Concr Res 42, 834-846 (2012).

[6] Pereira, E.B. and Fischer, G. and Barros, J.A.O. "Effect of hybrid fiber reinforcement on the cracking process in fiber reinforced cementitious composites" Cem Conc Comp 34, 1114-1123 (2012).

[7] Shah, S.P., "Experimental methods for determining fracture process zone and fracture parameters." *Eng Fract Mech* **35**:3-14 (1990).

[8] Chu, T.C., Ranson, W.F., Sutton, M.A., Peters, W.H., "Applications of digital-image-correlation techniques to experimental mechanics", *Exp Mech* **25**(3): 232-244 (1985).

[9] ASTM-E647, "Standard test method for measurement of fatigue crack growth rates." *ASTM International* (2005).

[10] Pereira, E.B., Fischer, G. and Barros, J.A.O., "Image-based detection and analysis of crack propagation in cementitious composites" *in* Leung, C.K.Y. (ed). *Proceedings of Advances in Concrete through Science and Engineering - RILEM*, Hong Kong, September 23-28 (2011).

[11] Pereira, E.B., Fischer, G. and Barros, J.A.O., "Near-tip analysis of crack propagation in cementitious composites" *in* Toledo-Filho, R.D. et al.(eds). *Proceedings of 2nd International RILEM Conference on Strain Hardening Cementitious Composites (SHCC2-Rio)*, Brazil, September 23-28 (2011).